
Chapter 7

*Co-doped TiO₂-ZrO₂
Composite*

7.1 Co-doped TiO₂-ZrO₂ Composite

The aim of this work is to primarily check the mixed oxides and the doped mixed for their performance as electrode in the DSSC. Hence, the structural and optical properties of mixed oxides in pure and doped form were studied extensively. However, there was a curiosity to know the effect of co doping on the characteristics of DSSC. With this in view a few samples were prepared with co doping to ascertain whether their structural and optical properties would not be adversely affected due to co doping. This pairs were made out of a transition and rare earth metal ions. Their structural and optical properties were studied using XRD and UV-Visible spectroscopy.

Shifting of optical absorption edge of TiO₂ to the visible light range with low recombination is one of the desirable properties of DSSC studies. To improve the photo absorption and charge separation properties of TiO₂, it can be co-doped by two metals [1-9]. Doping of two metals can produce disorders and which can affect the optical properties of TiO₂ [10-12]. The pairing of these metal ions was done with one metal ion from the transition or alkaline earth group and the other from the rare earth group. The transition/alkaline earth metals taken are Copper (Cu), Aluminium (Al), Zinc (Zn) and Manganese (Mn) while the rare earth co dopants are Cerium (Ce) and Europium (Eu). Hence, eight pair of dopants [(Cu, Ce) (Cu, Eu), (Al, Ce), (Al, Eu), (Zn, Ce), (Zn, Eu), (Mn, Ce) and (Mn, Eu)] were incorporated into the TiO₂-ZrO₂ mixed oxide samples.

7.2 Synthesis of Samples

Co-doped TiO₂-ZrO₂ composites were prepared by the hydrothermal method. TiO₂-ZrO₂ composites were doped with two metal ion combinations [(Al, Ce), (Al, Eu), (Cu, Ce), (Cu, Eu), (Zn, Ce), (Zn, Eu), (Mn, Ce) and (Mn, Eu)]. Titanium isopropoxide, Zirconium propoxide and isopropanol were used as starting chemicals. All chemicals were analytical grade and used as received. The synthesis was carried out as follows: Ti isopropoxide and Zr propoxide were diluted in isopropanol to obtain mixtures in a 7:3 TiO₂:ZrO₂ molar ratio. Dilute HNO₃ was added drop wise to the alkoxide solution kept under vigorous stirring in an ice bath. After alkoxide hydrolysis the alcogel was obtained. The alcogel was transferred to a stainless steel autoclave. The temperature was raised to 240 °C and the sample was maintained under autogenic pressure for 24 h. Then, the sample was oven-dried at 100 °C (2 h) and finally calcined at 450 °C for 4 hours under static air atmosphere. Mixed oxides in solid form were obtained.

7.3 Characterization of Samples

The structural properties and composition of prepared samples were analyzed by X-ray diffraction. The optical properties of the samples were investigated by UV-Visible spectroscopy.

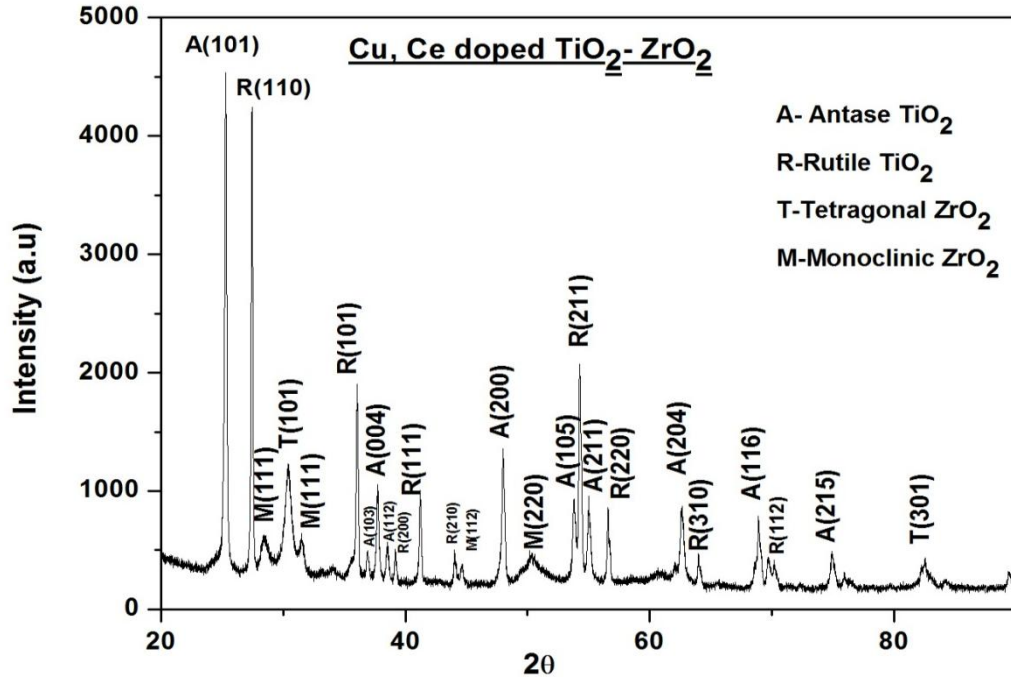
7.3.1 X-Ray Diffraction Analysis

The XRD patterns of the samples were recorded on Bruker D8 Advance X-ray diffractometer in 2θ range of 20° to 90° at room temperature. The XRD patterns of prepared samples are given in figure 1 to 8 and their structural parameters are given in Table 1 to 8.

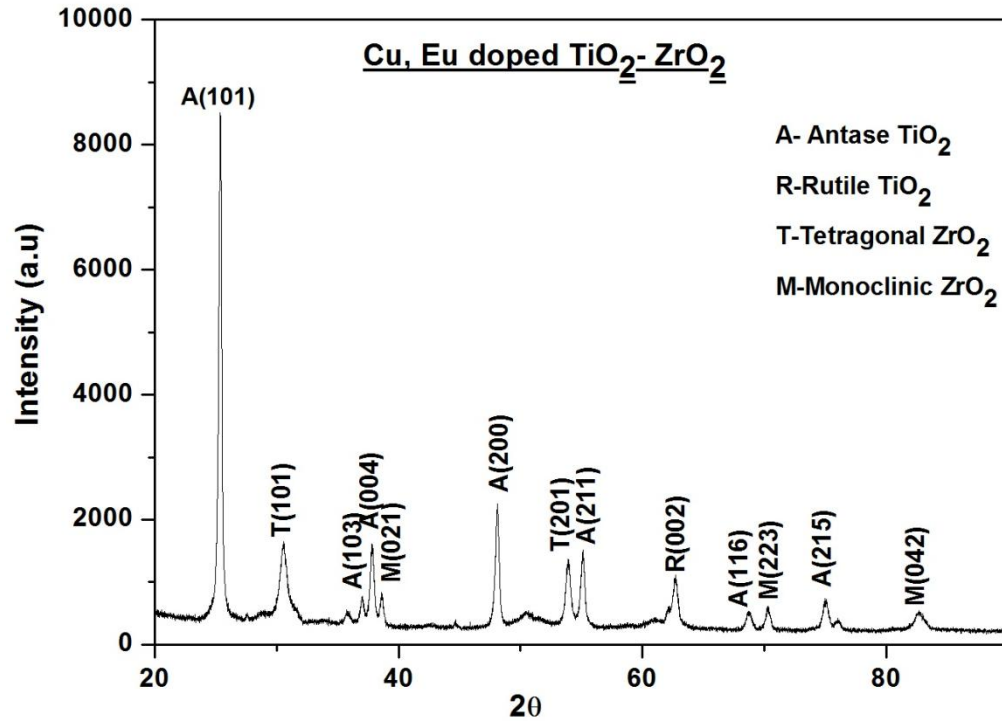
Highly intense peaks have been observed. The comparison of d values with JCPDS data base (Anatase TiO₂-21-1272, Rutile TiO₂-21-1276, Monoclinic ZrO₂-83-0944, and Tetragonal ZrO₂-79-1770) confirmed the presence of both oxides. The d values of all the peaks of the prepared sample match very closely with JCPDS data. For all samples peak at 2θ value of 25.25° has the highest intensity which is the characteristic peak of crystal plane (101) of Anatase TiO₂. TiO₂ was formed in purely Anatase phase i.e. 100% in the sample doped with Al, Ce.

The structural parameters of co-doped samples are given in Table 9. The average crystallite size for all the samples lies between 9.12 nm and 31.80 nm. It has been observed from the Table 9 that co-doping has increased the crystallite size to nearly that of undoped TiO₂-ZrO₂. Samples doped with Cu, Ce and Cu, Eu show highest crystallite size and crystallinity index. The similar ionic radii of Cu⁺² (0.073) and Zr⁺⁴ (0.072) can result into the Cu⁺² ion easily replacing Zr⁺⁴ ion, due to which the crystallization process is enhanced [13, 14]. The proper incorporation of Cu⁺² ion produces less strain this could be the reason for lowest strain value of Cu, Ce doped sample besides the high crystallite size. Sample doped with Cu, Ce shows lowest Anatase mass fraction of 45.87%. Generally the grain defect initiates phase transformation from Anatase to

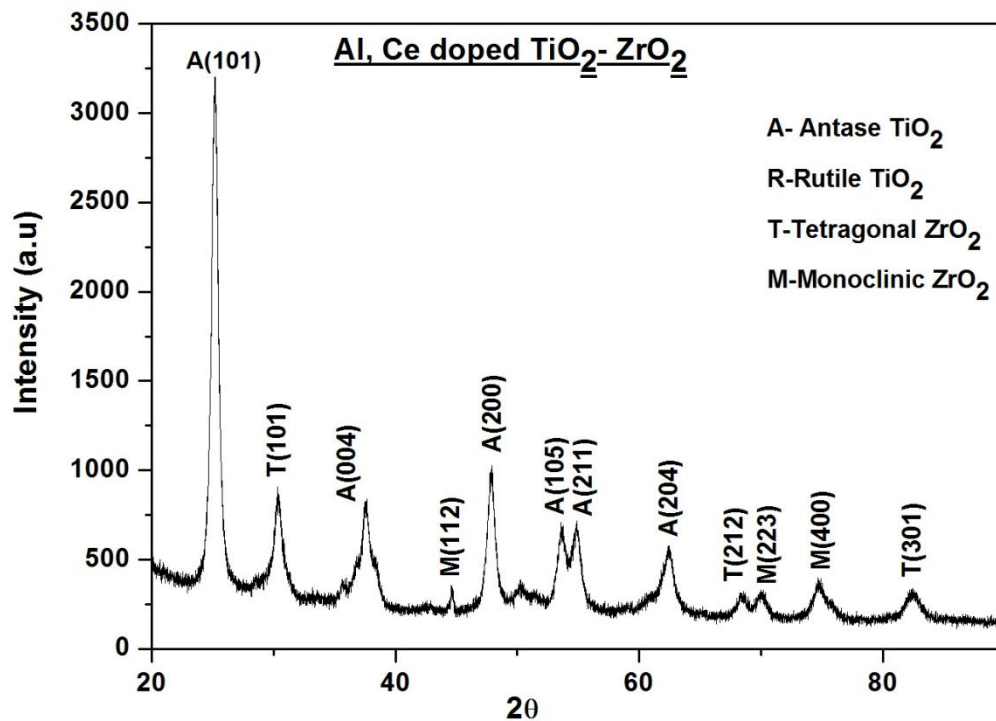
Rutile and reduces the strain [15]. The structural parameters of Cu, Ce doped sample shows good correlation among crystallite size, lattice strain and Anatase mass fraction. The lattice parameters are almost identical which shows formation of material with uniform crystal structure.

Figure 1: XRD pattern of sample Cu, Ce doped TiO₂-ZrO₂ compositeTable 1: Structural parameters of Cu, Ce doped TiO₂-ZrO₂ composite

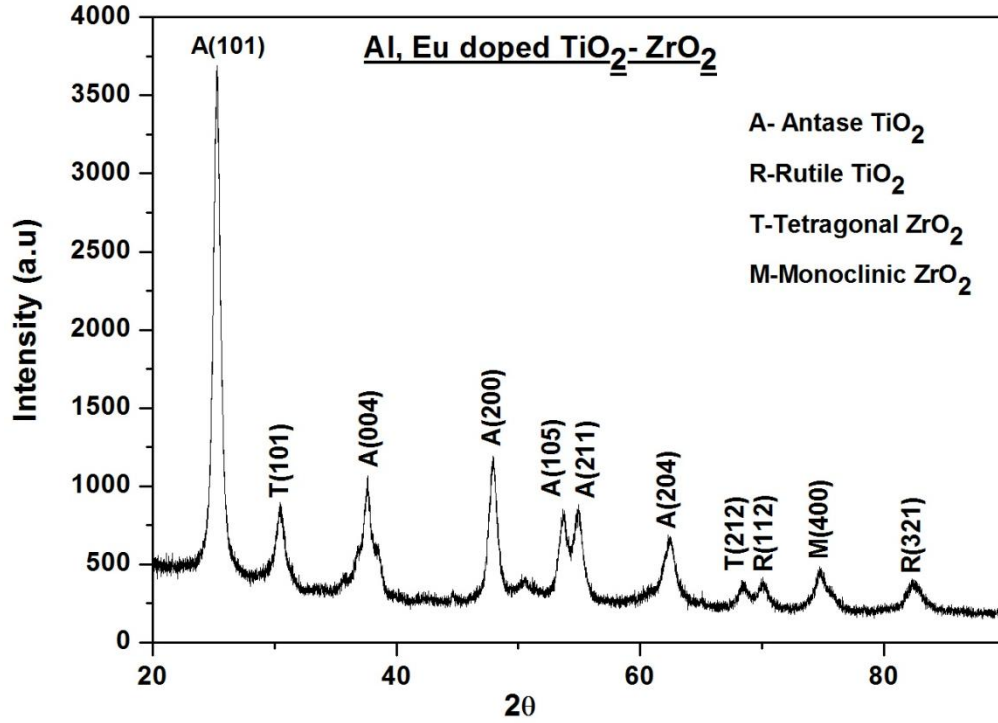
Experimental d values	JCPDS d values	Crystallite size (nm)	Strain (%)	Anatase content (%)
3.5186	3.52	43.82	0.015	
3.2468	3.247	51.77	0.012	
3.1373	3.1598	12.73	0.048	
2.9381	2.9529	15.30	0.037	
2.4883	2.4870	42.95	0.013	
2.4338	2.4310	35.62	0.012	
2.3808	2.3780	37.07	0.012	
2.3345	2.3320	37.93	0.010	
2.2981	2.2970	43.46	0.010	
2.1877	2.1880	42.80	0.011	
2.0541	2.0540	38.53	0.012	45.87
2.0285	2.0187	31.57	0.012	
1.8934	1.8920	31.91	0.060	
1.8158	1.8161	6.19	0.012	
1.7016	1.6999	26.56	0.009	
1.6881	1.6874	35.13	0.010	
1.6670	1.6665	32.64	0.008	
1.6244	1.6237	37.83	0.011	
1.4813	1.4808	27.56	0.008	
1.4533	1.4528	34.14	0.009	
1.3609	1.3641	29.81	0.011	
1.1673	1.1670	13.01	0.015	

Figure 2: XRD pattern of sample Cu, Eu doped TiO₂-ZrO₂ compositeTable 2: Structural parameters of Cu, Eu doped TiO₂-ZrO₂ composite

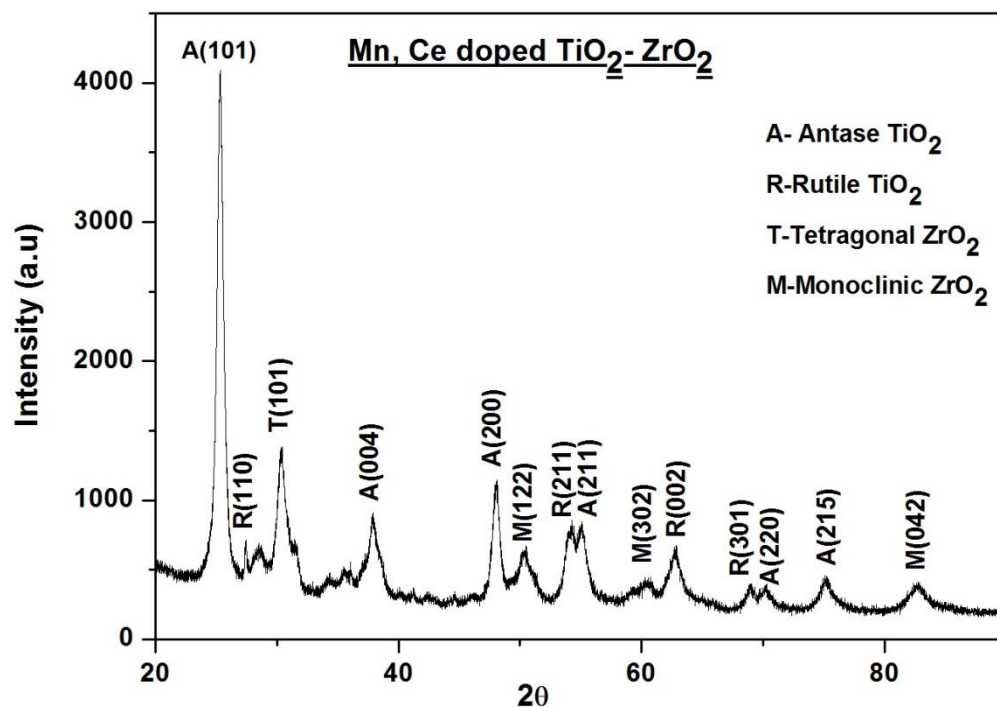
Experimental d values	JCPDS d values	Crystallite size (nm)	Strain (%)	Anatase content (%)
3.5072	3.52	30.06	0.022	85.80
2.9200	2.9529	12.63	0.045	
2.5080	2.5380	14.78	0.033	
2.4264	2.431	25.70	0.018	
2.3767	2.378	26.84	0.017	
2.3292	2.3292	35.88	0.012	
1.8887	1.8920	24.40	0.015	
1.6987	1.6999	20.62	0.016	
1.6642	1.6665	25.32	0.012	
1.4793	1.4797	18.37	0.015	
1.3647	1.3641	15.13	0.017	
1.3382	1.3381	20.69	0.012	
1.2647	1.2649	19.20	0.012	
1.1654	1.1646	12.23	0.018	

Figure 3: XRD pattern of sample Al, Ce doped TiO₂-ZrO₂ compositeTable 3: Structural parameters of Al, Ce doped TiO₂-ZrO₂ composite

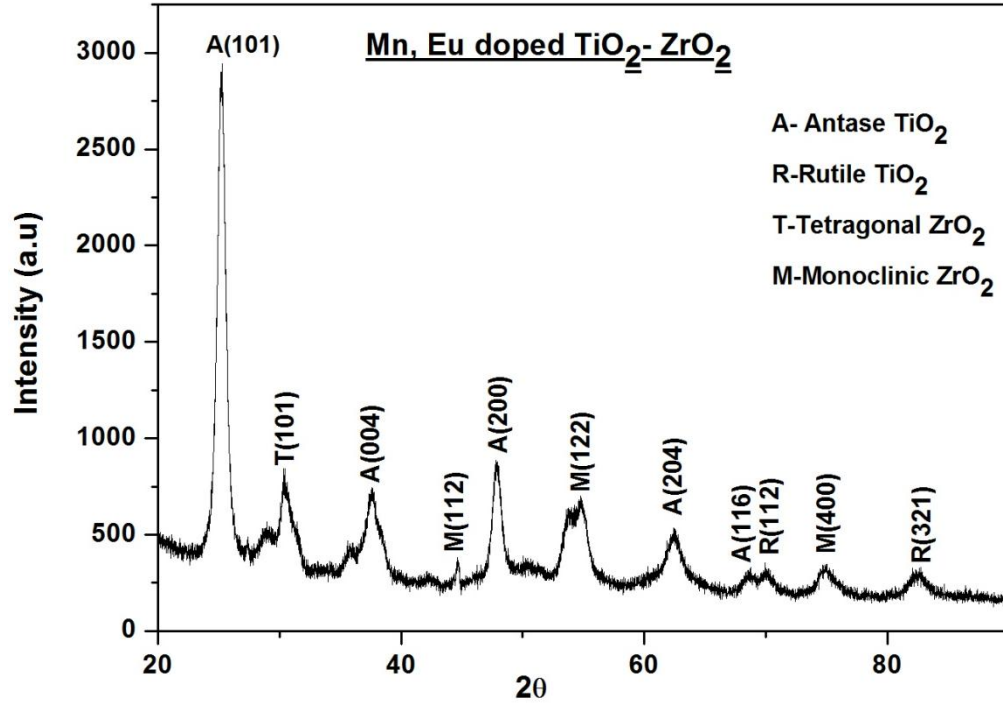
Experimental d values	JCPDS d values	Crystallite size (nm)	Strain (%)	Anatase content (%)
3.5324	3.52	13.50	0.051	100%
2.9444	2.9529	11.16	0.051	
2.3859	2.378	8.91	0.052	
1.8968	1.8920	11.60	0.032	
1.7080	1.6999	4.56	0.073	
1.4848	14808	8.31	0.035	
1.3670	1.3656	9.40	0.028	
1.3392	1.3381	7.94	0.033	
1.2696	1.2690	8.31	0.030	
1.1686	1.1670	8.14	0.028	

Figure 4: XRD pattern of sample Al, Eu doped TiO₂-ZrO₂ compositeTable 4: Structural parameters of Al, Eu doped TiO₂-ZrO₂ composite

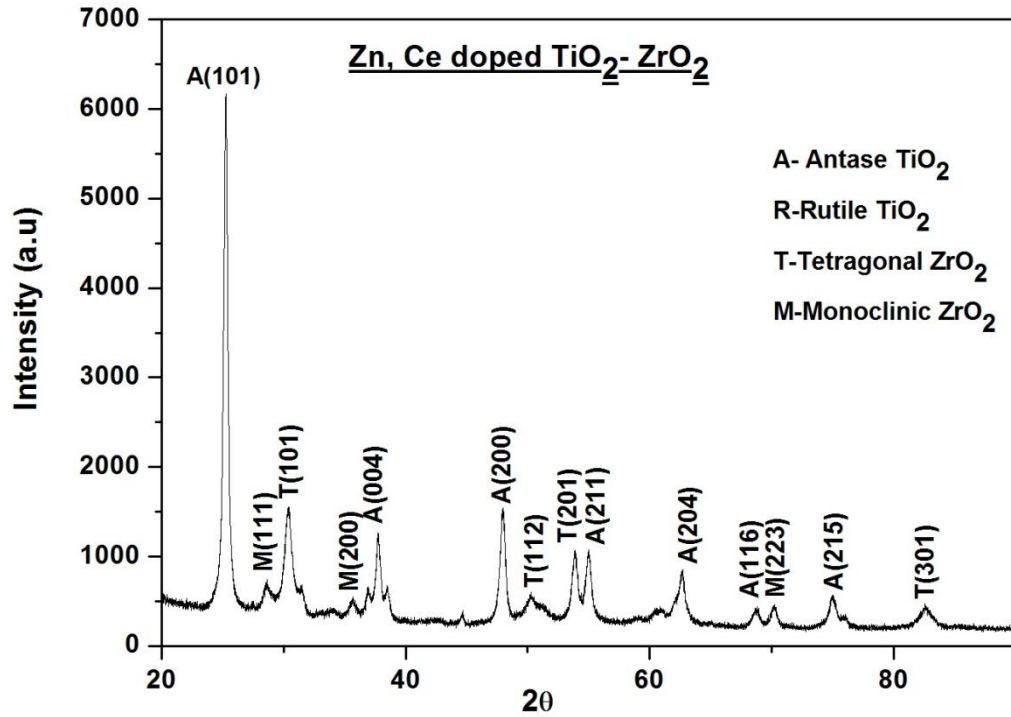
Experimental d values	JCPDS d values	Crystallite size (nm)	Strain (%)	Anatase content (%)
3.5209	3.52	12.69587	0.054	87.77
2.9333	2.9529	8.76599	0.065	
2.3864	2.378	9.50802	0.049	
1.8965	1.8920	10.81767	0.034	
1.7068	1.6999	9.27145	0.036	
1.6684	1.6665	9.48511	0.034	
1.4879	1.4808	7.61838	0.038	
1.3713	1.3656	9.56786	0.028	
1.3428	1.3480	9.89912	0.026	
1.2686	1.2690	8.65758	0.028	
1.1701	1.1702	6.92698	0.033	

Figure 5: XRD pattern of sample Mn, Ce doped TiO₂-ZrO₂ compositeTable 5: Structural parameters of Mn, Ce doped TiO₂-ZrO₂ composite

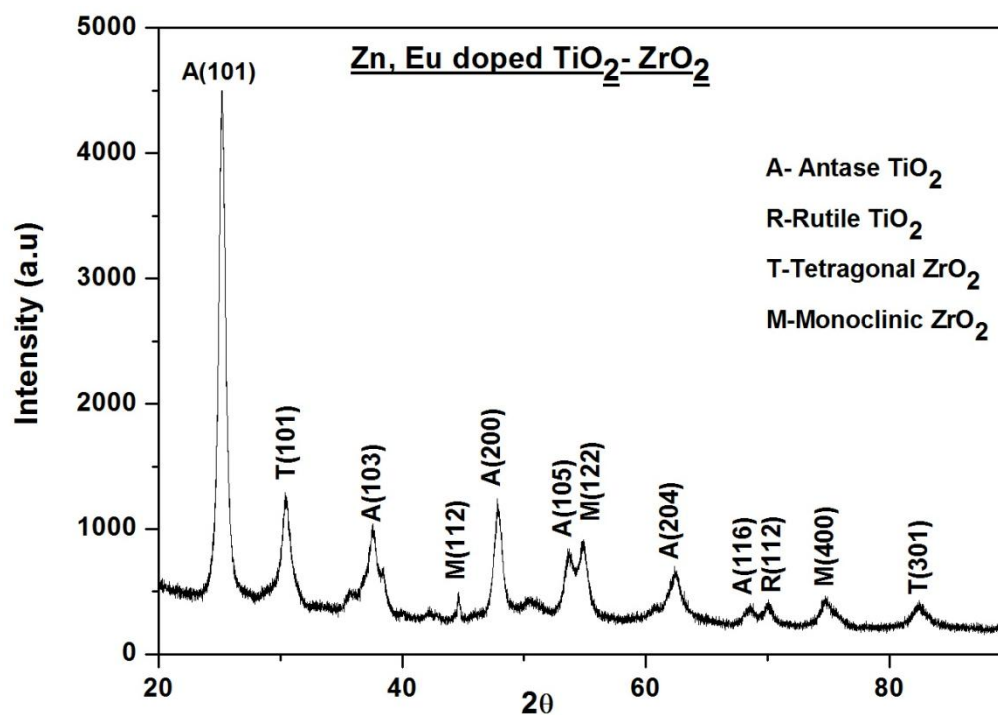
Experimental d values	JCPDS d values	Crystallite size (nm)	Strain (%)	Anatase content (%)
3.5118	3.51	13.69	0.050	82.97
3.2517	3.247	34.00	0.018	
3.1229	3.1598	9.76	0.062	
2.9420	2.9529	10.36	0.055	
2.3692	2.378	7.74	0.060	
1.8869	1.8920	12.55	0.029	
1.8051	1.8012	6.68	0.053	
1.6876	1.6874	4.90	0.067	
1.4790	1.4797	7.73	0.037	
1.3581	1.3598	4.71	0.056	
1.2638	1.2649	12.55	0.019	
1.1644	1.1646	7.84	0.029	

Figure 6: XRD pattern of sample Mn, Eu doped TiO₂-ZrO₂ compositeTable 6: Structural parameters of Mn, Eu doped TiO₂-ZrO₂ composite

Experimental d values	JCPDS d values	Crystallite size (nm)	Strain (%)	Anatase content (%)
3.5221	3.52	10.45	0.066	87.99
2.9349	2.9529	8.12	0.071	
2.3884	2.378	5.29	0.088	
2.0278	2.0187	28.37	0.014	
1.8999	1.8920	9.90	0.037	
1.6733	1.6752	4.54	0.072	
1.4854	1.4808	5.64	0.051	
1.3428	1.3378	5.63	0.046	
1.2696	1.2690	6.06	0.041	
1.1699	1.1702	7.22	0.031	

Figure 7: XRD pattern of sample Zn, Ce doped TiO₂-ZrO₂ compositeTable 7: Structural parameters of Zn, Ce doped TiO₂-ZrO₂ composite

Experimental d values	JCPDS d values	Crystallite size (nm)	Strain (%)	Anatase content (%)
3.5221	3.52	22.37	0.030	93.48
2.9460	2.9529	12.46	0.046	
2.5154	2.5380	11.13	0.044	
2.3828	2.378	19.18	0.024	
1.8956	1.8920	17.40	0.021	
1.8124	1.8141	6.26	0.056	
1.6985	1.6976	17.70	0.018	
1.6682	1.6665	15.88	0.020	
1.4800	1.4808	12.28	0.023	
1.3626	1.3641	13.15	0.020	
1.3381	1.3381	15.84	0.016	
1.2647	1.2649	13.26	0.018	
1.1669	1.1664	8.32	0.027	

Figure 8: XRD pattern of sample Zn, Eu doped TiO₂-ZrO₂ compositeTable 8: Structural parameters of Zn, Eu doped TiO₂-ZrO₂ composite

Experimental d values	JCPDS d values	Crystallite size (nm)	Strain (%)	Anatase content (%)
3.5266	3.52	13.27	0.052	89.72
2.9365	2.9529	9.59	0.060	
2.4018	2.431	4.44	0.106	
2.0292	2.0187	29.48	0.013	
1.8993	1.8920	12.08	0.030	
1.6712	1.6752	4.62	0.071	
1.4872	1.4808	7.00	0.041	
1.3623	1.3641	7.95	0.033	
1.3417	1.3465	8.04	0.032	
1.2688	1.2690	6.40	0.038	
1.1686	1.1670	5.80	0.039	

Table 9: Structural parameters of Co-doped TiO₂-ZrO₂ composite

Sample	Crystallite Size (nm)	Anatase Content	Strain	Crystallinity Index	Lattice Parameters	
					Anatase Phase	
					a	c
Cu, Eu TZ	21.56	85.8%	0.019	95.03%	3.78	9.51
Cu, Ce TZ	31.80	45.87%	0.017	91.59%	3.78	9.52
Al, Ce TZ	9.19	100%	0.041	88.95%	3.79	9.54
Al, Eu TZ	9.38	87.77%	0.039	86.04%	3.79	9.54
Mn, Ce TZ	11.05	82.97%	0.045	88.63%	3.77	9.47
Mn, Eu TZ	9.12	87.99%	0.052	86.35%	3.80	9.55
Zn, Ce TZ	14.25	93.48%	0.028	92.56%	3.79	9.53
Zn, Eu TZ	9.88	89.72%	0.047	88.64%	3.80	9.49

7.3.2 UV-Visible Spectroscopy

The absorption spectra of the samples were recorded on Thermo Fisher Scientific make Evolution 600 UV-Visible Spectrophotometer in the wavelength range of 200-900 nm. The optical bandgap was calculated by Tauc's plot. The absorption spectra and related Tauc's plot are shown in figure 9 to figure 16.

The optical parameters calculated from UV-Visible absorption spectra are given in Table 10. The following observations can be made from the results.

The absorption edge of all the samples lies below 500 nm. The peak absorption wavelengths vary in a range between 235 nm to 294 nm. Hence, there is no substantial change in the absorption pattern except that there is a shift towards lower wavelength.

The optical bandgap of all the samples lie between 3.00 eV to 3.45 eV. The bandgap values are on the higher side, compared to metal doped samples.

Figure 17 shows variation of absorption coefficient with wavelength. All the samples show higher absorption below 400 nm. After that, the absorption remains constant. Al, Ce doped TiO₂-ZrO₂ and Mn, Eu doped TiO₂-ZrO₂ samples shows relatively higher absorption.

Figure 18 shows variation of extinction coefficient with wavelength. The value of extinction coefficient is also higher for all the samples up to 400 nm, after which the value remains constant. The change in extinction coefficient for Mn, Ce doped TiO₂-ZrO₂ and Zn, Eu doped TiO₂-ZrO₂ samples is very small and remains almost uniform throughout the visible range.

The refractive index of the samples varies in a very short range from 2.26 to 2.36. Al, Eu doped TiO₂-ZrO₂ and Zn, Eu doped TiO₂-ZrO₂ samples show lowest and highest refractive index respectively.

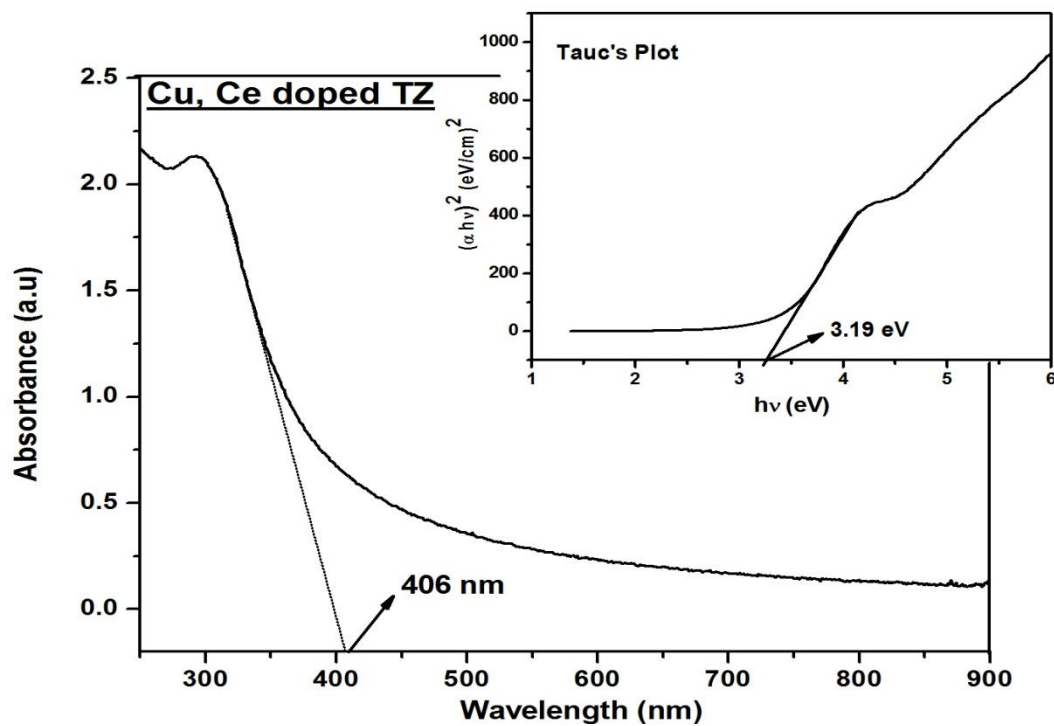


Figure 9: Absorption spectrum and Tauc's plot for Cu, Ce doped TiO₂-ZrO₂ composite

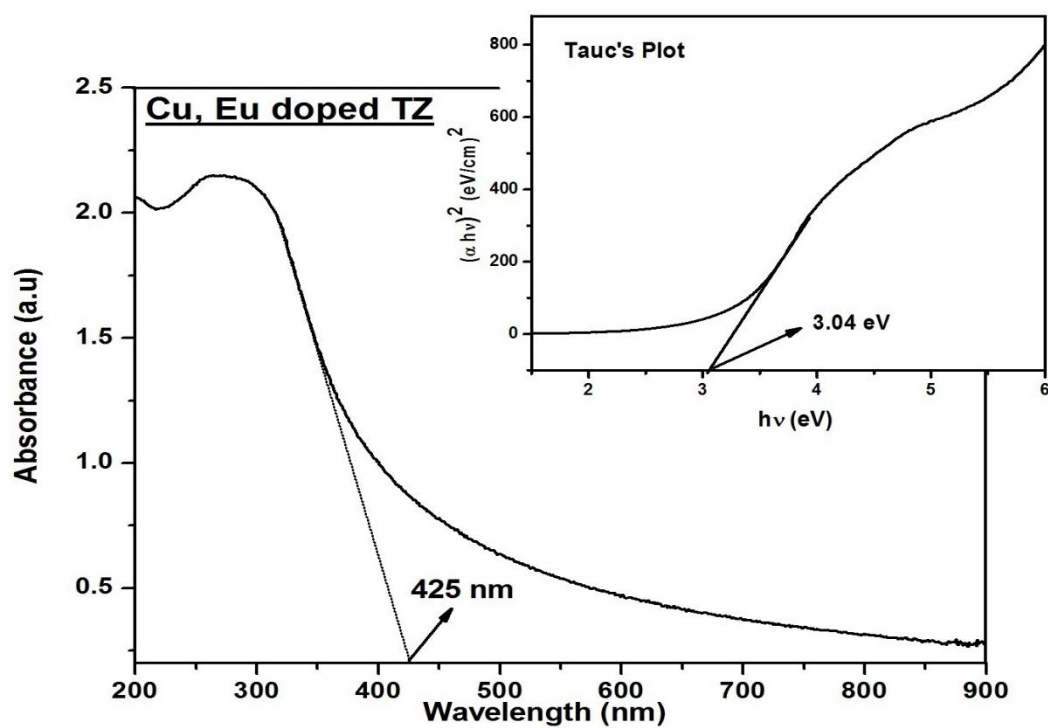


Figure 10: Absorption spectrum, and Tauc's plot for Cu, Eu doped TiO₂-ZrO₂ composite

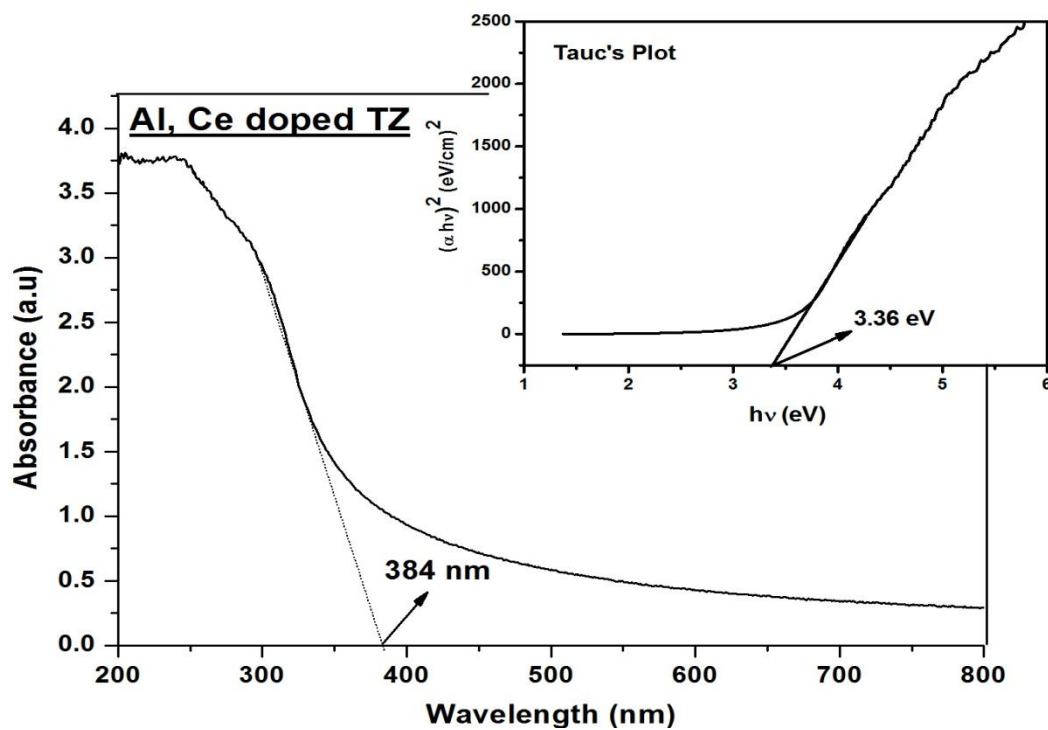


Figure 11: Absorption spectrum and Tauc's plot for Al, Ce doped TiO₂-ZrO₂ composite

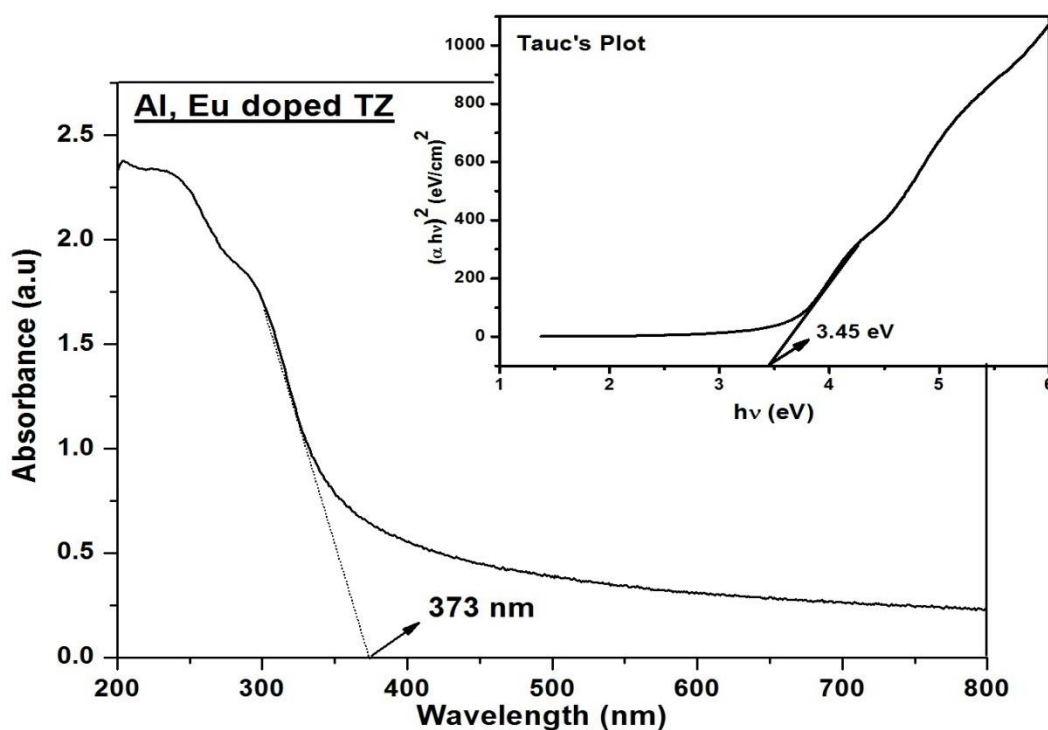


Figure 12: (a) Absorption spectrum and Tauc's plot for Al, Eu doped TiO₂-ZrO₂ composite

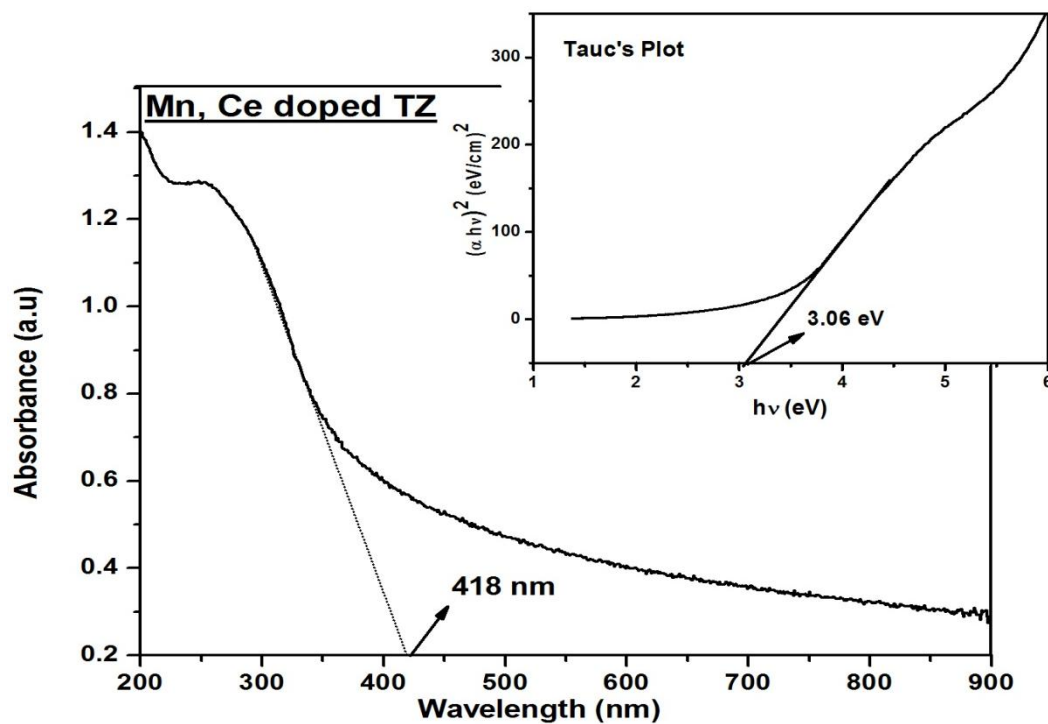


Figure 13: Absorption spectrum and Tauc's plot for Mn, Ce doped TiO₂-ZrO₂ composite

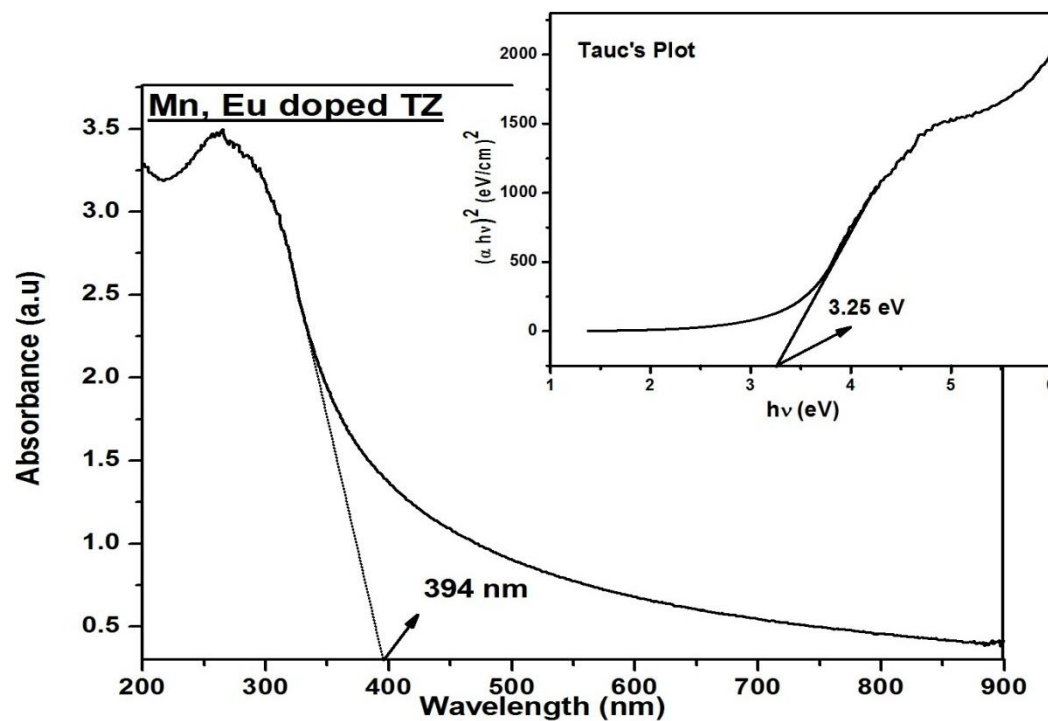


Figure 14: Absorption spectrum and Tauc's plot for Mn, Eu doped TiO₂-ZrO₂ composite

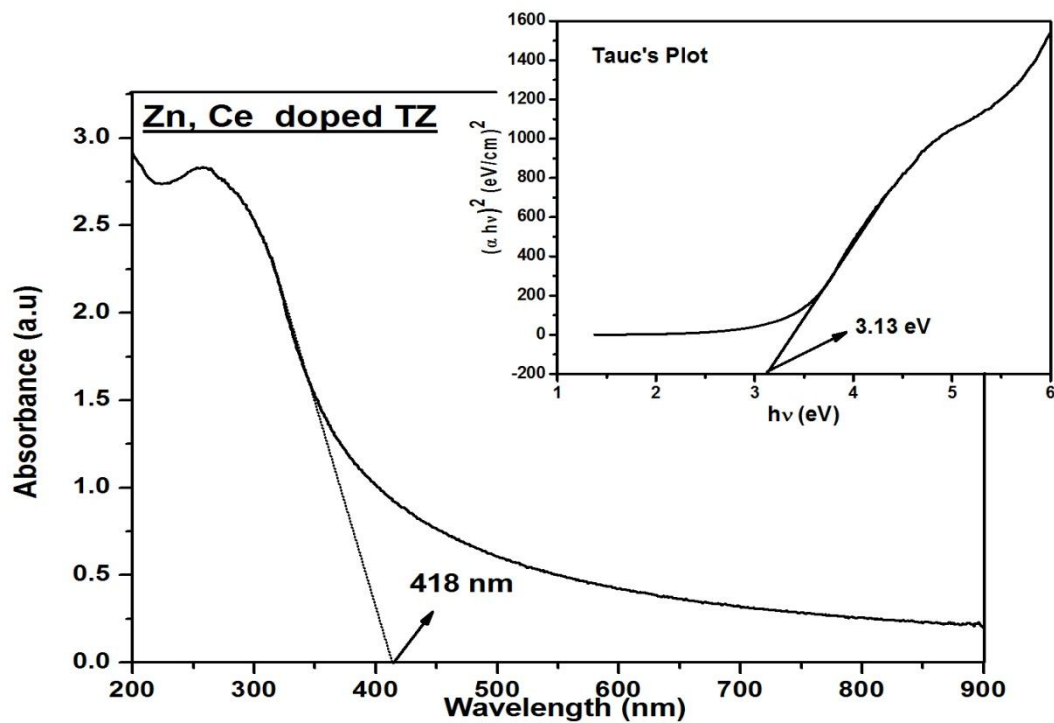


Figure 15: Absorption spectrum and Tauc's plot for Zn, Ce doped TiO₂-ZrO₂ composite

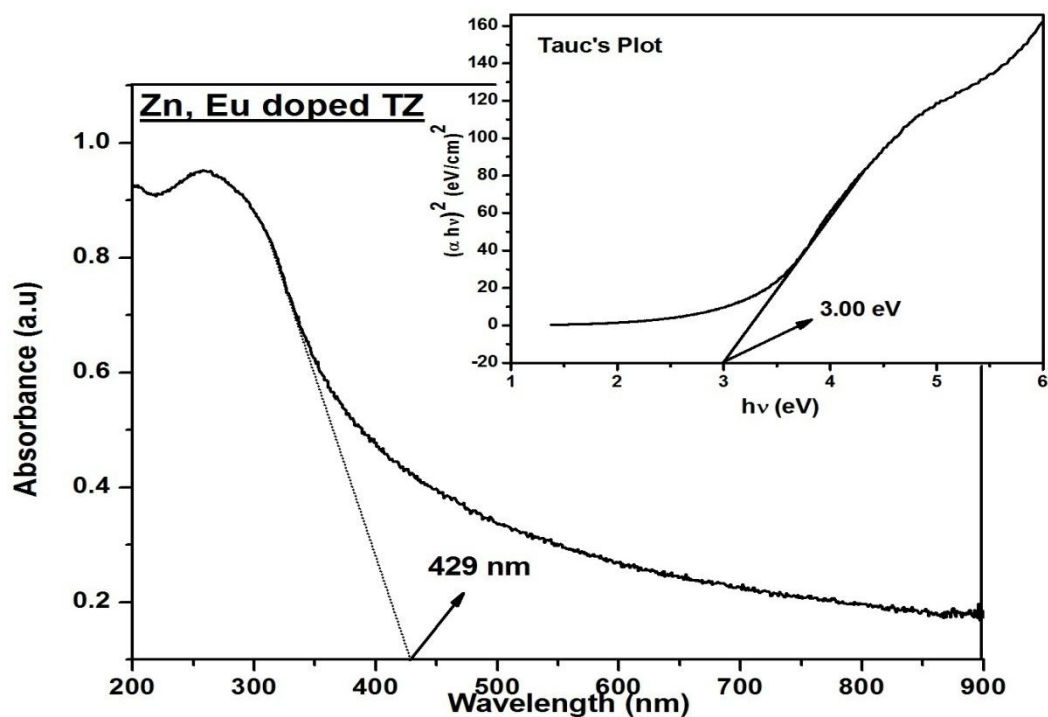


Figure 16: Absorption spectrum, and Tauc's plot for Zn, Eu doped TiO₂-ZrO₂ composite

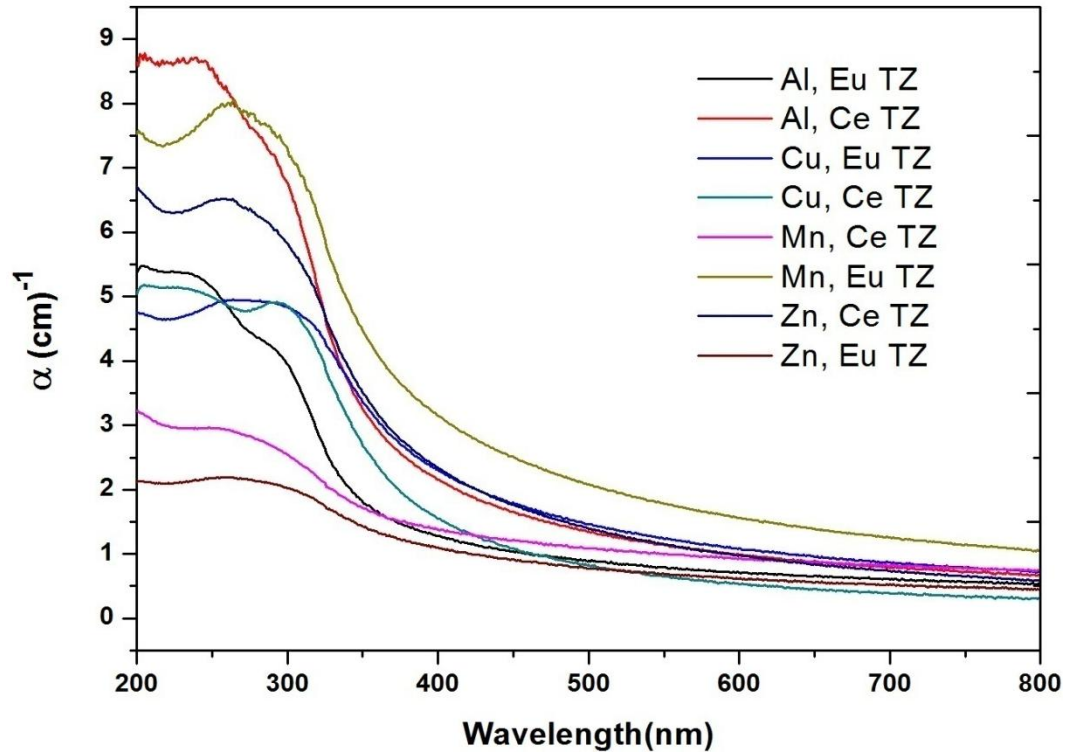


Figure 17: Variation of Absorption coefficient with wavelength

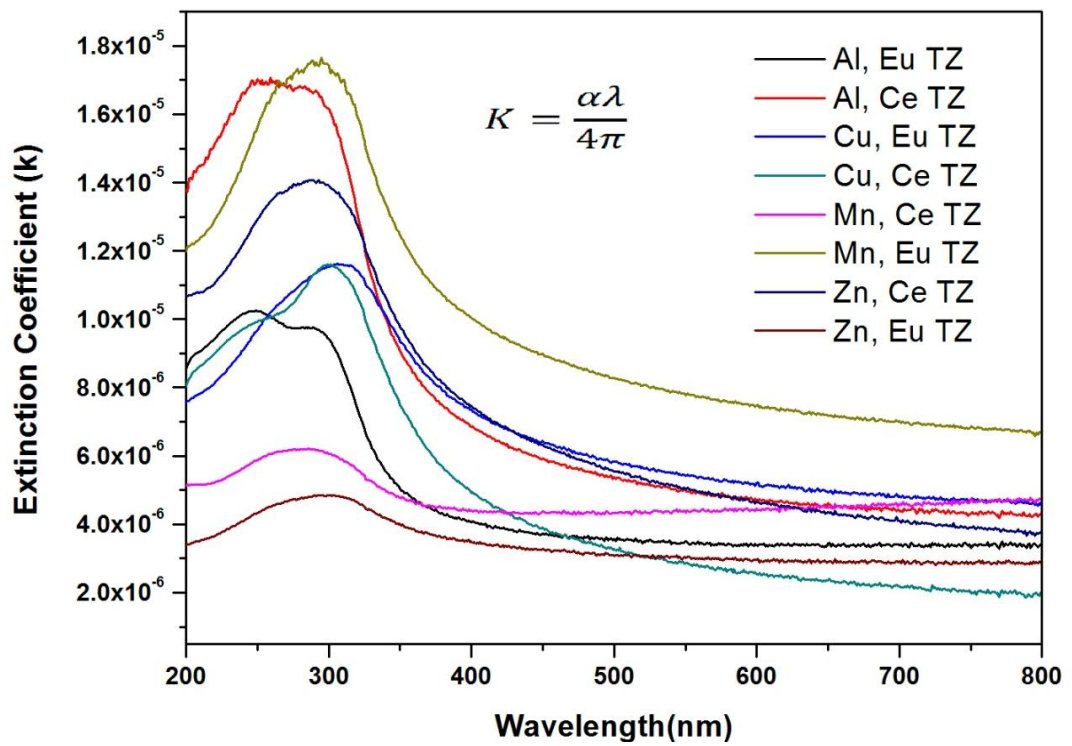


Figure 18: Variation of Absorption coefficient with wavelength

Table 10: Optical parameters of co-doped TiO₂-ZrO₂ samples

Sample	Peak Absorption	Optical Bandgap	Refractive Index
Cu, Ce doped TZ	294	3.19eV	2.31
Cu, Eu doped TZ	268	3.04 eV	2.35
Al, Ce doped TZ	237	3.36 eV	2.28
Al, Eu doped TZ	235	3.45 eV	2.26
Mn, Ce doped TZ	253	3.06 eV	2.34
Mn, Eu doped TZ	263	3.25 eV	2.30
Zn, Ce doped TZ	260	3.13 eV	2.33
Zn, Eu doped TZ	258	3.00 eV	2.36

7.4 Conclusion

Co-doped TiO₂-ZrO₂ samples were prepared using hydrothermal method. The XRD results revealed the formation of material as nano crystallite. The crystallinity of the material has increased. The average crystallite size was found to be between 9.19 nm and 31.80 nm. Formation of proper crystal structure is indicated from the low strain values and uniform lattice constant values. Anatase phase has been stabilized by co-doping and has increased substantially. The optical properties of material were analyzed by UV-Visible Spectroscopy. The optical bandgap of all the samples lie between 3.00 eV to 3.45 eV, which is higher compared to the single doped material.

References

- [1] X. Zhou, F. Peng, H. Wang, H. Yu, J. Yang, *J. Solid State Chem*, 2011, 184, 134–140.
- [2] X. Zhou, F. Peng, H. Wang, H. Yu, *J. Solid State Chem*, 2011, 184, 3002–3007.
- [3] N. Zhao, M. Yao, F. Li, F. Lou, *J. Solid State Chem*. 2011, 184, 2770–2775.
- [4] X. Yanga, F. Mab, K. Li, Y. Guob, J. Hub, W. Li, M. Huoa, Y. Guob, *J. Hazard. Mater*, 2010, 175, 429–438.
- [5] G. Li, D. Qu, W. Zhao, Y. Tong, *Electrochem. Commun*, 2007, 9, 1661–1666.
- [6] H. Serier, O. Toulemonde, D. Bernard, A. Demourgues, J. Majimel, M. Gaudon, *Mater. Res. Bull*, 2012, 47, 755–762.
- [7] Z. Wang, C. Chen, F. Wu, B. Zou, M. Zhao, J. Wang, C. Feng, *J. Hazard. Mater*, 2009, 164, 615–620.
- [8] H. Nian, S.H. Hahn, K. Koo, J.S. Kim, S. Kim, E.W. Shin, E.J. Kim, *Mater. Lett*, 2010, 64, 157–160.
- [9] C.C. Yen, D.Y. Wang, L.S. Chang, H.C. Shih, *J. Solid State Chem*, 2011, 184, 2053–2060.
- [10]. Ting C-C, Chen S-Y, Liu D-M, *J Appl Phys*, 2000, 88, 4628–4633.
- [11]. DeLoach JD, Scarel G, Aita CR, *J Appl Phys*, 1999, 83, 2377–2384.
- [12]. Tian J, Deng H, Sun L, Kong H, Yang P, Chu J, *Appl Surf Sci*, 2012, 258, 4893–4897.
- [13] Mahesh Bhagwata, A.V. Ramaswamy, A.K. Tyagib, Veda Ramaswamy, *Materials Research Bulletin*, 2003, 38, 1713–1724.

[14] Y. Kumar, M. A. Mohiddon, A. Srivastava, K. L. Yadav, *Ind. J. of Engg. And Mat. Sci*, 2009, 16, 390-394.

[15] Biswajit Choudhury and Amarjyoti Choudhury, *International Nano Letters*, 2013, 3, 55.